RAPID COMMUNICATIONS

PHYSICAL REVIEW B **94**, 201408(R) (2016)

Hyperfine-controlled domain-wall motion observed in real space and time

John N. Moore,[1] Junichiro Hayakawa,[1] Takaaki Mano,[2] Takeshi Noda,[2] and Go Yusa[1,*]

[1]*Department of Physics, Tohoku University, Sendai 980-8578, Japan*

[2]*National Institute for Materials Science, Tsukuba, Ibaraki 305-0047, Japan*

(Received 14 September 2016; revised manuscript received 23 October 2016; published 15 November 2016)

We perform real-space imaging of propagating magnetic domains in the fractional quantum Hall system using spin-sensitive photoluminescence microscopy. The propagation is continuous and proceeds in the direction of the conventional current, i.e., opposite to the electron flow direction. The mechanism of motion is shown to be connected to polarized nuclear spins around the domain walls. The propagation velocity increases when nuclei are depolarized, and decreases when the source-drain current generating this nuclear polarization is increased. We discuss how these phenomena may arise from spin interactions along the domain walls.

DOI: 10.1103/PhysRevB.94.201408

I. INTRODUCTION

Research around magnetic domains and their dynamics has become increasingly relevant, driven by the hunt for domain-based logic and memory [1,2]. These technologies could dramatically reduce device heating while increasing speed. A number of scientifically innovative methods for controlling the propagation of ferromagnetic domain walls have recently been pioneered [3–8]. Across these works numerous interaction phenomena have been identified as driving and assisting domain propagation, ranging from spin-transfer torques from injected electrons and optical pulses, to torques and stabilizing influences from Rashba fields and Dzyaloshinskii-Moriya interactions. Apart from these interactions, another potential control parameter relevant to domain motion is hyperfine interaction.

Coupling between conduction electrons and a material's nuclear spin bath has been known since the 1950's to occur via hyperfine interaction [9]. Recently, nuclear magnetic resonance (NMR) studies in semiconductors have attracted renewed interest for their value in research on quantum information processing, especially in quantum confined nanostructures [10–20]. It has been reported that electron-nuclear spin coupling can lead to dynamic nuclear polarization and sometimes can function as a good control parameter to manipulate electron spins [13,14], or may cause nuclear polarization to act back on the electronic system in complex ways [15–19]. One system in which hyperfine interaction becomes relevant is the fractional quantum Hall (FQH) system [10], where strongly interacting electrons condense into a two-dimensional (2D) liquid at fractional values of the Landau level filling factor ν [21]. At certain values of ν and magnetic field B, this system plays host to a phase transition between two degenerate spin-resolved many-bodied ground states, i.e., ferromagnetic and nonmagnetic states, in which electron spin polarization P is 1 and 0, respectively. Near this phase transition, bringing the system out of equilibrium with a strong source-drain current can excite into existence stripe-shaped domains, which elongate along the Hall electric field (perpendicular to the source-drain current direction); spin-resolved electrons passing between these domains undergo flip-flop scattering with nuclei, producing nuclear spin polarization P_{N} near domain walls [22]. In this Rapid Communication, we investigate the hyperfine-mediated controllability of domain walls in real space and time.

II. MEASUREMENTS

Using spin-sensitive photoluminescence (PL) microscopy, we image domains propagating through the sample in response to a direct source-drain current I_{dc}. This propagation is continuous and unidirectional. The propagation velocity increases when nuclei are resonantly depolarized, and it shows dependencies on ν and the magnitude of I_{dc} that also suggest P_{N}'s tendency to reduce the velocity. We discuss how these phenomena may arise from spin interactions along the domain walls.

Measurements were carried out at temperature $T \sim 60$ mK in a 15-nm-wide GaAs/AlGaAs quantum well sample containing a FQH liquid with ν close to $\frac{2}{3}$ and at the critical magnetic field ($B = 6.8$ T) of the $\nu = \frac{2}{3}$ spin phase transition [24]. An n-doped GaAs substrate functions as a back gate and enables us to tune two-dimensional electron density n_e and ν at constant B. The sample was measured by scanning optical microscopy and spectroscopy. We spatially mapped the integrated PL intensity produced by singlet-state charged excitons [25,26]; this intensity is primarily anticorrelated with the local P [24], but also is sensitive to the local P_{N} [22]. Accordingly, the nonmagnetic and ferromagnetic domains are distinguished by strong and weak PL intensities, respectively [24]. For comparison to the previous study [22], we applied a 13-Hz *alternating* source-drain current $I_{\mathrm{ac}} = 60$ nA to the sample near the phase transition [Fig. 1(b)]. Upon applying the current, the striped domains that are excited tend to be unstable for the first ~1 h; after this period they appear static over the duration of the imaging (~20 h). The spatial image at $\nu = 0.664$ [Fig. 1(b)] excited by I_{ac} is consistent with that reported earlier showing the formation of domain structures [22].

When, in contrast, *a direct* source-drain current I_{dc} is applied, the scenario is altered dramatically; the domains propagate spatially [Fig.s 2(a)–2(h); see the video in the Supplemental Material]. In Fig. 2(a), a domain wall in the right of the image at an arbitrary time $t = 0$ propagates 3–4 μm to the left at $t = 4.1$ min [Fig. 2(c)]. Another domain wall propagates across the image in the same manner [Figs. 2(d)–

[*]yusa@tohoku.ac.jp

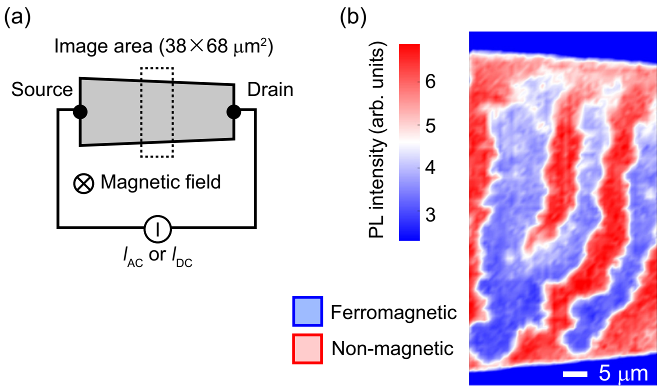

FIG. 1. (a) Schematic of the sample. Alternating (I_{ac}) or direct (I_{dc}) current can be applied between the source and drain. External magnetic field B perpendicular to the 2D electrons is 6.8 T throughout. (b) 38×68-μm^2 spatial image showing integrated PL intensity of a charged exciton singlet peak, at $\nu = 0.666$, with 13-Hz, $I_{ac} = 60$ nA alternating source-drain current. Image step size: 781 nm. $T \sim 60$ mK unless otherwise specified.

2(g)]. The propagation direction is identical to the current direction, and reversing the current direction reverses the propagation direction. The widths of these striped domains are consistently preserved [23], indicating that the domain walls all have nearly equivalent velocities, possibly because conservation of P throughout the system is energetically favorable.

The integrated microscopic PL (μ-PL) intensity obtained from a diffraction limited spot ($\phi \sim 1$ μm) at a fixed point under $I_{dc} = 110$ nA oscillates reasonably periodically in time with a period on the order of ~10 min [Fig. 3(a)], suggesting that the stripe domains form with a fairly equally spaced period. In contrast, for $I_{dc} = 0$ nA, all the imaged area contains a ferromagnetic ground state, and the PL intensity at the fixed point is constant over time. The averaged PL intensity for $I_{dc} = 0$ nA, denoted by a dotted line in Fig. 3(a), is near the center of oscillations observed for $I_{dc} = 110$ nA. The drops in intensity below this ferromagnetic ground-state value indicate the influence of P_N antiparallel to B inside of ferromagnetic phase domains. The increases in intensity above the ground-state value are due to the combined influence of P_N parallel to B and the vanishing of P in the nonmagnetic phase domains.

In order to obtain the average domain velocity along the horizontal direction $\upsilon_{\mathrm{domain}}$, we measured μ-PL intensities at two points (points 1 and 2) aligned along the length of the Hall bar [Fig. 3(c)]. In this measurement, the μ-PL spectrum was collected for 4 s at point 1; the measurement position was then immediately shifted 4 μm to the right (point 2) and the μ-PL spectrum was again collected for 4 s; after returning to the original point (point 1), the cycle was repeated. A time delay appears in the intensity at these two points due to the domain motion, and its average value can be determined from the cross correlation between the two sets of oscillations. The cross correlation is maximum at a time lag of -1.330 min [Fig. 3(d)]. The average velocity of the domains $\upsilon_{\mathrm{domain}}$, at $I_{dc} = 110$ nA, $\nu = 0.662$, thus, is estimated to be ~45 nm/s. The strong cross correlation confirms that the widths of the striped domains are preserved over short distances on the order of the domain widths.

To investigate the influence of nuclear spins on the domain motion, we depolarized nuclear spins by applying rf radiation through a two-turn coil wrapped around the sample. $\upsilon_{\mathrm{domain}}$ increases when rf is applied to resonantly depolarize the ^{75}As nuclei that have been polarized by I_{dc} (Fig. 4). We applied rf over a range of powers, both resonantly (red) and off resonantly (blue). The resonance and off-resonance frequencies were determined from the optically detected NMR spectrum taken in this sample at the same B [22]. There is a velocity difference of 30–40 nm/s between the two frequency cases, independent of rf power, P_{rf} (Fig. 4), which clearly indicates that polarized nuclear spins hamper domain motion and that $\upsilon_{\mathrm{domain}}$ can be increased by *resonantly* decreasing P_N. $\upsilon_{\mathrm{domain}}$ for both cases increases monotonically with P_{rf}. We attribute this increase to the temperature increase (Fig. 4 inset), which also has the tendency to reduce P_N via the thermal energy ($k_B T \sim 5.2$ μeV for 60 mK, where k_B is the Boltzmann constant). This energy can *nonresonantly* decrease P_N because of the small Zeeman energy of nuclear spins (~0.2 μeV and ~0.4 for ^{75}As and ^{71}Ga, respectively, at $B = 6.8$ T).

$\upsilon_{\mathrm{domain}}$ is also a function of ν [Fig. 5(a)]. $\upsilon_{\mathrm{domain}}$ is smallest near the phase transition ($\nu = \frac{2}{3}$) and is increased by detuning ν away from $\frac{2}{3}$. Given that P_N tends to slow down the propagation, the minimum in $\upsilon_{\mathrm{domain}}$ seen near to the phase transition is expected because P_N is generated most effectively near the phase transition. I_{dc} also influences $\upsilon_{\mathrm{domain}}$ [Fig. 5(b)]. The tendency for monotonic decrease in $\upsilon_{\mathrm{domain}}$ with increasing I_{dc} can be explained by the increase

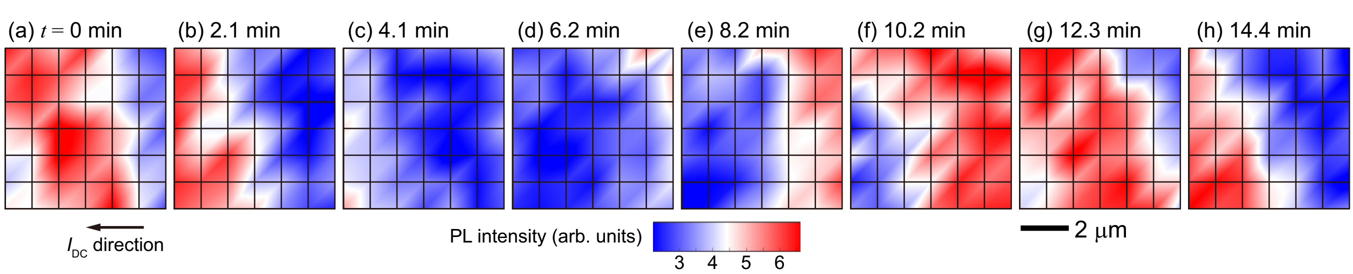

FIG. 2. 6×6-μm^2 PL-intensity images taken at the center of the region shown in Fig. 1(b) for t of (a) 0, (b) 2.1, (c) 4.1, (d) 6.2, (e) 8.2, (f) 10.2, (g) 12.3, and (h) 14.4 min. Each image is interpolated from 49 data points located at the crosses of the displayed 1-μm grid. Data points were measured vertically beginning at the top left and ending at the bottom right. There was a time interval of ~14 s between the collection of each image. Each image took ~110 s to collect. $I_{dc} = 110$ nA, $\nu = 0.664$. See video in the Supplemental Material [23].

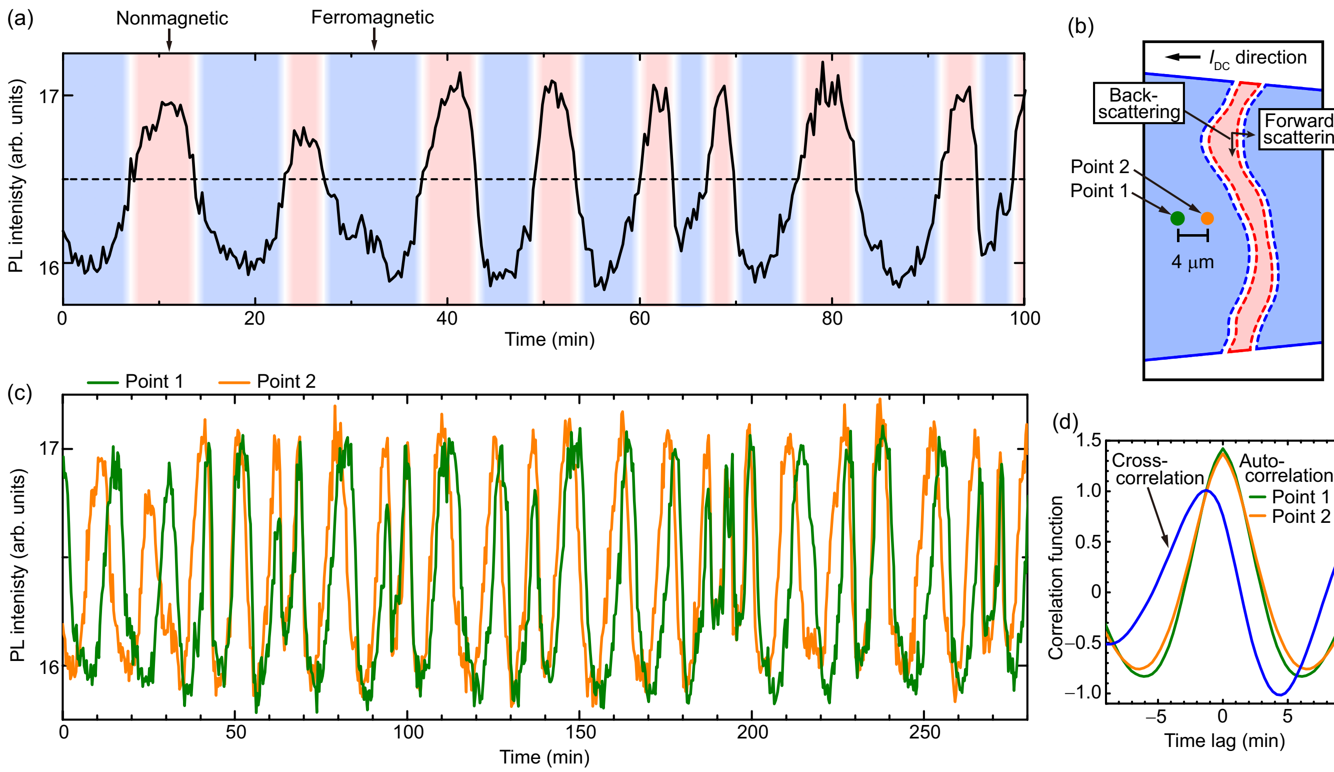

FIG. 3. (a) μ-PL intensity at fixed point as function of time with arbitrary $t = 0$, $I_{\mathrm{dc}} = 110$ nA; $\nu = 0.662$. The horizontal dotted line corresponds to intensity when $I_{\mathrm{dc}} = 0$ nA. (b) Schematic of sample describing locations of points 1 and 2. Solid and dotted lines denote edge channels and backscattering paths, respectively. (c) μ-PL intensity as a function of time at points 1 (green) and 2 (orange) in the same conditions as (a). (d) Autocorrelation functions of PL intensity at points 1 (green) and 2 (orange), and cross-correlation function between PL intensity at points 1 and 2 (blue) as a function of time lag.

in P_{N} generated by the current. Later, we will also discuss other possible mechanisms which may account for this behavior.

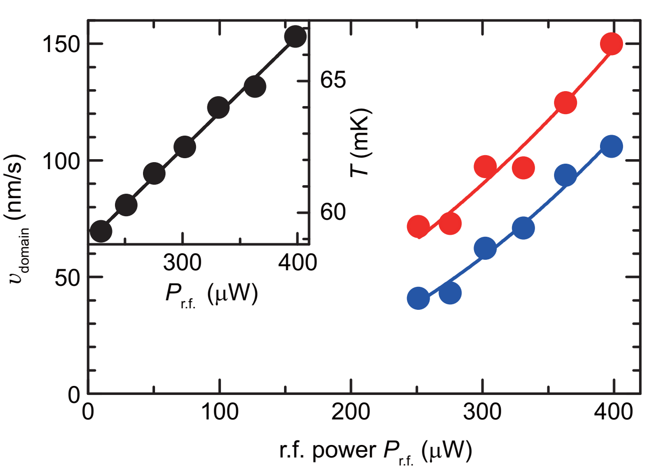

FIG. 4. Average domain velocity in I_{dc} direction $\upsilon_{\mathrm{domain}}$ as a function of on-resonant (red, 49.7717 MHz) and off-resonant (blue, 49.84 MHz) rf power P_{rf}; $I_{\mathrm{dc}} = 110$ nA, $\nu = 0.664$. Inset: The dilution refrigerator mixing chamber temperature T as a function of P_{rf}.

III. DISCUSSION

The low speed of these domains is noteworthy. Under the alternating current condition used for Fig. 1(b), the current direction alternates with a 77-ms period, and the domain propagation length for one half-cycle is order estimated to be 1–10 nm. This is negligibly small compared to the domain size; thus, the images under alternating current here appear static [Fig. 1(b)] [22].

Comparison of $\upsilon_{\mathrm{domain}}$ to the velocity of the current is important. The velocity of edge current υ_{edge} [*along* the

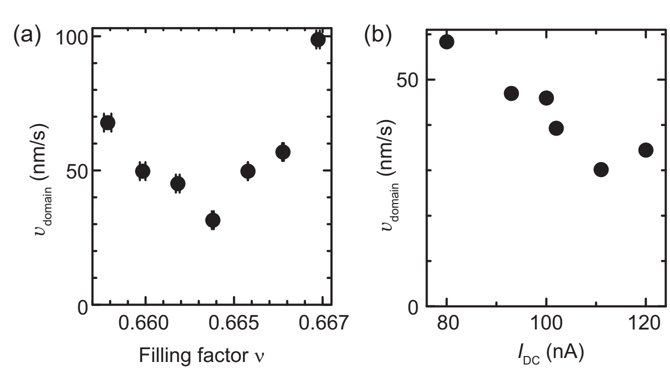

FIG. 5. (a) $\upsilon_{\mathrm{domain}}$ as a function of ν; $I_{\mathrm{dc}} = 110$ nA. Error in ν calculated from uncertainty in electron density. (b) $\upsilon_{\mathrm{domain}}$ as a function of I_{dc}; $\nu = 0.664$.

solid blue and red lines in Fig. 3(b)] is order estimated to be $\upsilon_{\text{edge}} \sim \frac{I_{\text{dc}}}{e n_e \ell_B} \sim 10^5$ m/s, where $n_e \sim 10^{11}$ cm^{-2}, e is the elementary charge, and ℓ_B is the magnetic length. Electrons contributing to I_{dc} must pass as charge current across the domain walls bridging the two sides of the Hall bar, i.e., forward scattering at the domain walls. The average velocity $\upsilon_{\text{forward}}$ of the forward scattering [*across* the *dotted* blue and red lines in Fig. 3(b)], i.e., the charge current across a domain wall, is roughly $\upsilon_{\text{forward}} \sim \frac{\ell_B}{W}\upsilon_{\text{edge}} \sim 10^2$ m/s, where W ($\sim$60 μm) is the width of the Hall bar, assuming a uniform current distribution over the domain wall [27]. υ_{domain} ($\sim 10^{-7}$ m/s) is, therefore, >9 orders of magnitude slower than the velocity of the charge current ($\sim 10^2$ m/s). This and the direction of the source-drain current indicate that the domain propagation does not assist in the charge transport. Further, it appears likely that the domain motion does not in itself cause *any* charge transport, but rather is the result of the domain interfaces propagating through a medium of static electron spins.

For this type of propagation to occur, electrons located along the spin phase interfaces must undergo spin flips. Given the observed propagation speed, the average amount of time it takes an electron at an interface to flip its spin is order estimated to be $\sim$2 s [28]. The experiments reported here conclusively draw a link between this spin flip rate and the nuclear polarization; however, it is difficult to be certain of the detailed mechanism responsible for this. We offer here some considerations.

To begin, the propagation direction is opposite to that caused by the spin-torque transfer mechanism. Thus, an alternative interaction must be the cause of the domain-wall motion here. Spin-torque transfer cannot be ruled out, however, as a possible explanation of the decrease in υ_{domain} with increasing I_{dc} [Fig. 5(b)], as this may reflect spin-torque transfer trying to move the domains in the opposite direction to the observed propagation.

One mechanism which might seem to provide an intuitive explanation involves the P_{N} generated by the current as the driving force [29]. P_{N} modifies the local electron spin splitting energy [30], and as a result, both magnetic phases become more energetically favorable in the regions along the side of the domain walls where P_{N} is generated, i.e., the side "downstream" of electron flow. This creates a local perturbation of the domain wall as electrons inside join the favorable phase, displacing the interface. A continued cycle of P_{N} generation and interface displacement causes an effective motion of the domain walls in the upstream direction, as observed. However, this mechanism of motion is contradicted by the observation of P_{N} slowing down the domain velocity (Fig. 4).

The domain motion can also be accounted for by steps in the electrochemical potential which are formed by the backscattering channels located along the domain walls. Electronic spin states located on the upper step along each boundary are unstable and may reduce their potential energy by flipping their spins to join the adjacent spin phase. Since no electrons are transported in this process, the domain wall is displaced in the upstream direction. As ν is moved away from the phase transition, states in the domain walls become less stable owing to the larger energy gap between the phases [31], and electron spins may flip more readily, causing υ_{domain} to grow away from the transition as observed in Fig. 5(a).

The decrease in υ_{domain} with P_{N} can be accounted for, but it requires a mechanism in which P_{N} is able to diffuse across the phase boundaries, which is a process that is thought to be inhibited by electronic spin states making up the domain walls. Because of its direction of polarization, P_{N} that diffuses across the boundaries acts to decrease the number of nuclei available for electron spin flip-flop exchange processes. Thus, electron spins on the upstream side of domain walls will flip less frequently, and the domain-wall motion will be slowed.

ACKNOWLEDGMENTS

The authors are grateful to N. Shibata, K. Muraki, and T. Fujisawa for discussions, and to Y. Hirayama and M. Matsuura for experimental support. This work was supported by the Mitsubishi Foundation and a Grant-in-Aid for Scientific Research (No. 24241039) from the Ministry of Education, Culture, Sports, Science, and Technology (MEXT), Japan. J.N.M. was supported by a Grant-in-Aid from MEXT and the Marubun Research Promotion Foundation. J. H. was supported by a Grant in-Aid from the Tohoku University International Advanced Research and Education Organization.

[1] D. A. Allwood, G. Xiong, C. C. Faulkner, D. Atkinson, D. Petit, and R. P. Cowburn, Science **309**, 1688 (2005).

[2] S. S. P. Parkin, M. Hayashi, and L. Thomas, Science **320**, 190 (2008).

[3] M. Yamanouchi, D. Chiba, F. Matsukura, and H. Ohno, Nature (London) **428**, 539 (2004).

[4] A. Yamaguchi, T. Ono, S. Nasu, K. Miyake, K. Mibu, and T. Shinjo, Phys. Rev. Lett. **92**, 077205 (2004).

[5] I. M. Miron, T. Moore, H. Szambolics, L. D. Buda-Prejbeanu, S. Auffret, B. Rodmacq, S. Pizzini, J. Vogel, M. Bonfim, A. Schuhl, and G. Gaudin, Nat. Mater. **10**, 419 (2011).

[6] S. Emori, U. Bauer, S.-M. Ahn, E. Martinez, and G. S. D. Beach, Nat. Mater. **12**, 611 (2013).

[7] J. H. Franken, M. Herps, H. J. M. Swagten, and B. Koopmans, Sci. Rep. **4**, 5248 (2014).

[8] A. J. Ramsay, P. E. Roy, J. A. Haigh, R. M. Otxoa, A. C. Irvine, T. Janda, R. P. Campion, B. L. Gallagher, and J. Wunderlich, Phys. Rev. Lett. **114**, 067202 (2015).

[9] G. Feher, Phys. Rev. Lett. **3**, 135 (1959).

[10] S. Kronmüller, W. Dietsche, K. von Klitzing, G. Denninger, W. Wegscheider, and M. Bichler, Phys. Rev. Lett. **82**, 4070 (1999).

[11] T. Machida, T. Yamazaki, K. Ikushima, and S. Komiyama, Appl. Phys. Lett. **82**, 409 (2003).

[12] G. Yusa, K. Muraki, K. Takashina, K. Hashimoto, and Y. Hirayama, Nature (London) **434**, 1001 (2005).

[13] J. R. Petta, A. C. Johnson, J. M. Taylor, E. A. Laird, A. Yacoby, M. D. Lukin, C. M. Marcus, M. P. Hanson, and A. C. Gossard, Science **309**, 2180 (2005).

[14] F. H. L. Koppens, J. A. Folk, J. M. Elzerman, R. Hanson, L. H. Willems van Beveren, I. T. Vink, H. P. Tranitz, W. Wegscheider,

L. P. Kouwenhoven, and L. M. K. Vandersypen, Science **309**, 1346 (2005).

[15] K. Ono and S. Tarucha, Phys. Rev. Lett. **92**, 256803 (2004).

[16] G. Yusa, K. Hashimoto, K. Muraki, T. Saku, and Y. Hirayama, Phys. Rev. B **69**, 161302(R) (2004).

[17] C. Latta, A. Hgele, Y. Zhao, A. N. Vamivakas, P. Maletinsky, M. Kroner, J. Dreiser, I. Carusotto, A. Badolato, D. Schuh, W. Wegscheider, M. Atature, and A. Imamoglu, Nat. Phys. **5**, 758 (2009).

[18] I. T. Vink, K. C. Nowack, F. H. L. Koppens, J. Danon, Y. V. Nazarov, and L. M. K. Vandersypen, Nat. Phys. **5**, 764 (2009).

[19] S. Hennel, B. A. Braem, S. Baer, L. Tiemann, P. Sohi, D. Wehrli, A. Hofmann, C. Reichl, W. Wegscheider, C. Rössler, T. Ihn, K. Ensslin, M. S. Rudner, and B. Rosenow, Phys. Rev. Lett. **116**, 136804 (2016).

[20] H. Sanada, Y. Kondo, S. Matsuzaka, K. Morita, C. Y. Hu, Y. Ohno, and H. Ohno, Phys. Rev. Lett. **96**, 067602 (2006).

[21] D. C. Tsui, H. L. Stormer, and A. C. Gossard, Phys. Rev. Lett. **48**, 1559 (1982).

[22] J. N. Moore, J. Hayakawa, T. Mano, T. Noda, and G. Yusa, arXiv:1606.06416.

[23] See Supplemental Material at http://link.aps.org/supplemental/10.1103/PhysRevB.94.201408 for a video on domain propagation in 6×6-μm^2 PL-intensity images from an arbitrary time $\tau = 0$–204 min. $I_{\rm dc} = 110$ nA, $\nu = 0.664$. Image step size: 1 μm. Some of the frames of this video are displayed in Fig. 2.

[24] J. Hayakawa, K. Muraki, and G. Yusa, Nat. Nanotechnol. **8**, 31 (2013).

[25] G. Yusa, H. Shtrikman, and I. Bar-Joseph, Phys. Rev. Lett. **87**, 216402 (2001).

[26] A. Wójs, A. Gładysiewicz, and J. J. Quinn, Phys. Rev. B **73**, 235338 (2006).

[27] $\upsilon_{\rm edge}$ is the velocity through a cross section $\sim\ell_B$, whereas $\upsilon_{\rm forward}$ is the velocity through the cross section $\sim W$. Thus, $\upsilon_{\rm forward}$ is $\frac{\ell_B}{W}$ times smaller than $\upsilon_{\rm edge}$, because of the charge conservation law.

[28] With an electron density of $\sim 1 \times 10^{11}$ cm^{-2}, the area occupied per electron is $\sim 1 \times 10^3$ nm^2. Taking a domain velocity of 30 nm/s, all the electrons along the domain interface must switch to the phase of the adjacent domain at a rate of ~ 1 time per second. Since only half of these electrons will undergo a spin flip, the average time for a given electron at the interface to flip its spin is ~ 2 s.

[29] Flip-flop scattering produces $P_{\rm N}$ pointing downward (upward) with respect to B after electrons participating in the direct current cross domain walls and join the ferromagnetic (nonmagnetic) phase.

[30] $E_{\rm S} = |g^*|\mu_{\rm B} B - A\langle I_z \rangle$, where g^* is the effective g factor of electrons, $\mu_{\rm B}$ is the Bohr magneton, $A > 0$ is the hyperfine constant, and $\langle I_z \rangle$ is the average of the nuclear spin quantum number.

[31] N. Shibata and K. Nomura, Phys. Soc. Jpn. **76**, 103711 (2007).